Investigation of Free Volume, Interfacial, and Toughening Behavior for Cyanate Ester/Bentonite Nanocomposites by Positron Annihilation

D. H. Yu,[1] B. Wang,[1] Y. Feng,[2] Z. P. Fang[2]

[1]*Department of Physics, Wuhan University, Wuhan 430072, China*
[2]*Institute of Polymer Composites, Zhejiang University, Hangzhou 310027, China*

Received 19 January 2006; accepted 15 March 2006
DOI 10.1002/app.24428
Published online in Wiley InterScience (www.interscience.wiley.com).

ABSTRACT: Effects of filler on microstructure and toughening behavior of cyanate ester (CE)/bentonite (BT) nanocomposites with different content of BT have been studied by positron annihilation lifetime spectroscopy, X-ray diffraction, transmission electron microscopy, dynamic mechanical analysis, etc. The interesting results found by PALS indicate that the size and concentration of the free volume holes and the apparent free volume fraction increased with increasing the content of BT, which indicates that adding nano-layers to thermosetting materials can lead to the high crosslinking density structure ''looser.'' The experimental results reveal that the increases in size of free volume holes and apparent free volume fraction are related to the increasing conversion of cure reaction. On the other hand, the mechanism of toughening (by adding the nano-clay to the thermosetting material) has been discussed by combining free volume and interfacial property. It is shown that, for the high crosslinking thermosetting material-based nanocomposites, both the property of free volume and dispersion state of nano-layers are the two key factors in determining toughening property. © 2006 Wiley Periodicals, Inc. J Appl Polym Sci 102: 1509–1515, 2006

Key words: positron annihilation; free volume; nanocomposites; structure–property relations; toughness

INTRODUCTION

Cyanate ester (CE) resins have been the important thermosetting materials since they were first synthesized in 1960s for their attractive physical, mechanical, and electrical properties,[1,2] such as high modulus, high glass transition temperature (T_g: 250–290°C),[3] low dielectric constant (2.5–3.1 MHz),[3] good radar transparency,[1] very low moisture absorption (0.6–2.5%),[3] etc. Consequently, CE resins have been widely applied in electronics, aerospace, adhesion, and miscellaneous applications nowadays.[1]

CE monomers undergo cyclotrimerization reaction to product a triazine ring connecting unit, as shown in Scheme 1, and then form a three-dimensional crosslinking structure. That is why the CE resins have excellent properties as mentioned above. However, like most high crosslinking thermosetting materials, low toughness is their main drawback, which limited their further applications. It still requires suitable modification to improve their toughness without reducing the intrinsic physical strength for structural applications.[3]

Correspondence to: B. Wang (bwang@positron.whu.edu.cn).
Contract grant sponsor: National Natural Science Foundation of China.

Accordingly, many efforts were devoted to improve the toughness of CE, such as the preparation of flexibilized cyanate resins, the incorporation of monocyanates, the utilization of rubber toughening technologies, the use of organic-clay toughening and the preparation of semi-interpenetrating networks (SIPNs), etc, which have been proven to be very useful.[4] However, toughening usually occurs at the expense of other characteristics of the CE resin. In recent years, one of the most effective methods is to prepare the nanocomposite materials by introducing the nanoscale layered silicate into the matrix, such as layered silicates and clays. Polymer/layered nanocomposite have attracted a great deal of attention, because these nanocomposites exhibit marked improvement in physical and chemical properties compared with pure polymers.[5] Bentonite (BT) is a kind of naturally abundant clay. It has been applied in numerous industrial fields due to its good performance-cost ratio. The outstanding feature of BT is that the silicate layers can be expanded and even delaminated by organic molecules under proper condition.[6,7] For their high polarity, monocyanate can easily diffuse into the organic modified BT clay galleries. The polarity of the group —OCN is thought to promote diffusion into the clay (modified by organic amine) galleries. The maximum layer expansion is obtained when intragallery polymerization rates exceed that in the extragallery regions allowing exfoliation before gelation.[3] An unbalance

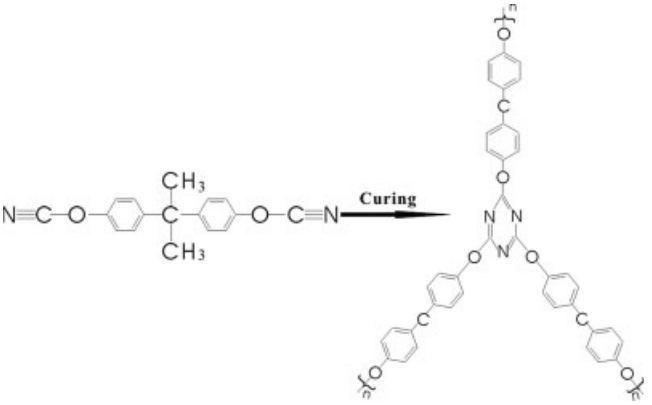

Scheme 1 Cyclotrimerization of cyanante esters.

between these rates assures the formation of an exfoliated structure. Although, this method to prepare the CE/clay nanocomposites has been elucidated to some extent,[3,8–10] the crosslinking structure of these materials, especially the three-dimensional structure, has not yet been clearly clarified, which must be understood concerning their modifications and applications. On the other hand, the mechanism of toughening using layered silicates is not very clear, unlike the case of using rubber to improve its toughness, in which the phase separation plays the key role. Therefore, characterization of the microstructure of the CE/BT nanocomposites not only can direct the modification of CE, but also has significant theoretical meaning.

Positron annihilation lifetime spectroscopy has been used as a unique technology to probe the free volume properties of polymers for many years.[11,12] PALS was proven to be sensitive to atom-scale free volume holes of polymers, due to the formation of the positronium (Ps) atom, which is a bound state of e^+ and e^-. There are two kinds of Ps atoms. The *para*-positronium (*p*-Ps), in which the spins of the positron and electron are antiparallel, has a lifetime of 0.125 ns by self-annihilation in vacuum; while the *ortho*-positronium (*o*-Ps), in which the spins of the positron and electron are parallel, has a longer lifetime of 142 ns in vacuum.[13] However, in polymers the *o*-Ps atoms are preferentially localized in the atom-scale holes and their lifetime is shortened to about 1–5 ns by the pick-off annihilation with an electron from the surrounding molecules. The *o*-Ps lifetime τ_3 directly correlates to the size of free volume holes and its intensity I_3 contains information about the free volume concentration.[13] The relationship between the *o*-Ps lifetime τ_3 and the radius of the free volume hole (R) has been established by an empirical equation:[14]

$$\tau_3 = \frac{1}{2}\left[1 - \frac{R}{R+\Delta R} + \frac{1}{2\pi}\sin\frac{2\pi R}{R+\Delta R}\right]^{-1} \quad (1)$$

where R is the radius of the free volume hole, ΔR (=1.656 Å) is derived from fitting the observed *o*-Ps lifetimes in molecular solids with known hole sizes. Furthermore, the fractional free volume f is evaluated in terms of the *o*-Ps intensity I_3 and the size of free volume hole ($V = \frac{4}{3}\pi R^3$):

$$f = CVI_3 \quad (2)$$

where C is a constant. Usually, we use apparent free volume fraction, f_{app}:

$$f_{app} = VI_3 \quad (3)$$

because what we concerned is not the absolute value of free volume fraction, but instead the variation of free volume fraction.[12]

In this study, the PALS is used to investigate the changes of the free volume size, the concentration, and the apparent free volume fraction in CE/BT nanocomposites with different content of BT. On the basis of previous results,[8] we studied the effects on microstructure of CE by BT layers from the aspect of free volume, and further discussed the mechanism of toughening by adding BT into CE system.

EXPERIMENTS

Sample preparation

A phenolic-based cyanate ester (CE) resin (melting point: 79°C, molecular weight: 278, purity > 98%, which was supplied by Jinan Special Structure Institute of China Aero-Industry) and the organically modified bentonite (NH_3^+-BT) were used. Organically modified bentonite (BT, Code: NB905) was obtained from the Zhejiang Huate Group, Hangzhou, China, which was ion-exchanged with octadyl trimethyl ammonium. The CE resin was placed in a beaker maintained at 90°C. A high-shear mixing blade was placed into the resin and stirred. BT (1 and 2.5 wt %) was then slowly added in and mixed for 15 min. The cure schedule was: heat to 120–150°C over 30 min in vacuum, then ramp to 160°C and hold for 1 h; then 180°C/1 h, 200°C/1 h, 220°C/1 h, 240°C/1 h, and 260°C/1 h.[8]

Complementary characterization

X-ray diffraction (XRD) was performed in a Rigaku D/Max-2550PC system with Eulerian 1/4 cradle and Cu Kα radiation (40 kV, 40 mA, λ = 1.540E), 2°/min.

Transmission electron microscopy (TEM) was taken by a JEM-1200EX electronic microscope, Japan.

Dynamic mechanical analysis (DMA) was performed using a DMA Q800 V3.13 Build 74 by TA Instruments, USA, which was carried out in dual cantilever bending mode at a vibration frequency of 1 Hz in the temperature range from 40 to 250°C, and the heating rate was 2°C/min.

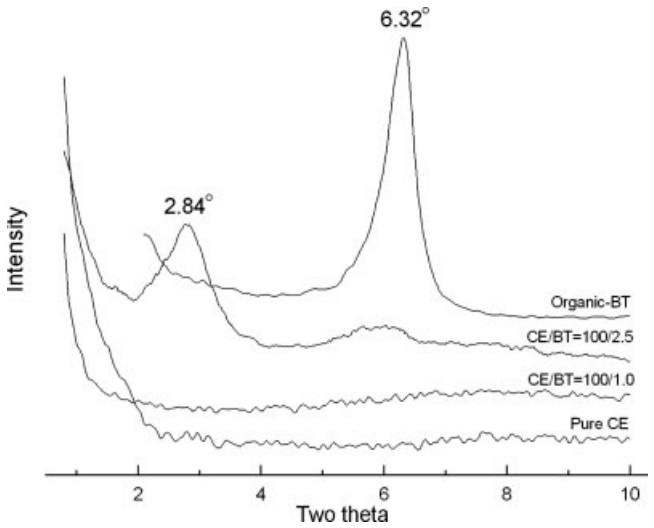

Figure 1 XRD patterns of BT and CE/BT nanocomposites.

The impact test was performed according to GB/T2571-1995 (similar to ISO179-1993) on an XCJ-4 Charpy impact instrument at (23 ± 2)°C. The results of the impacting test were obtained by averaging the results of above five measurements.

Positron annihilation lifetime spectroscopy

A 30 μCi ^{22}Na positron source sealed between two sheets of Ni foil (1 mg/cm^2) was sandwiched between two identical samples. A conventional fast-fast coincident lifetime spectrometer is used for PALS measurement at room temperature. The time resolution is found to be a sum of two Gaussians with $FWHM_1$ = 280 ps (90%) and $FWHM_2$ = 320 ps (10%). Each spectrum contained ~10^6 counts.

RESULTS AND DISCUSSION

In this article, all the positron lifetime spectra are resolved into three components using the program PATFIT.[15] All the variations of the fit (χ^2) were smaller than 1.2. The two short components $\tau_1 \approx 0.12$–0.15 ns and $\tau_2 \approx 0.30$–0.40 ns are attributed to the self-annihilations of *para*-positronium (*p*-Ps) and ''free'' positron annihilation in the bulk state, and are found to exhibit no correlation with the free volume properties,[16] but the second component (τ_2 and its intensity I_2) contains the structure information of interfacial layers.[17] The longest lifetime component $\tau_3 \approx 1.2$–3.0 ns is assigned to the *o*-Ps pick-off annihilation in the free volume holes in polymers, which correlated with the properties of free volume holes.

Structure of nanocomposites

Generally, the structural characteristics of polymer-layered nanocomposites can typically been measured by XRD analysis and TEM observation. By monitoring the position, shape, and intensity of the basal reflections from the distributed silicate layers, the nanocomposites structure (intercalated or exfoliated) may be identified.[18] Figure 1 illustrates the comparison of the XRD patterns of BT (organic modified BT) and CE/BT nanocomposites with different content of BT. For the pure CE, there are no reflections. For the pure organic modified BT, there was a reflection peak at $2\theta \approx 6.32^\circ$ (*d*-spacing = 1.397 nm). For the nanocomposite with 1 wt % BT, the reflection peak disappeared. From the corresponding TEM picture in Figure 2(a), we can observe the exfoliated and intercalated (the dark lines) BT layers. But, the exfoliation is the main phase. Combining the TEM picture with XRD pattern, we can see that the exfoliation of BT is dominative in this sample (1 wt % BT) and that the disordered structure is formed. For the nanocomposite with 2.5 wt % BT, the broad reflection peak located at $2\theta = 2.84^\circ$ (*d*-spacing = 3.11 nm), which indicates that the CE has been intercalated into the galleries and the distance between silica

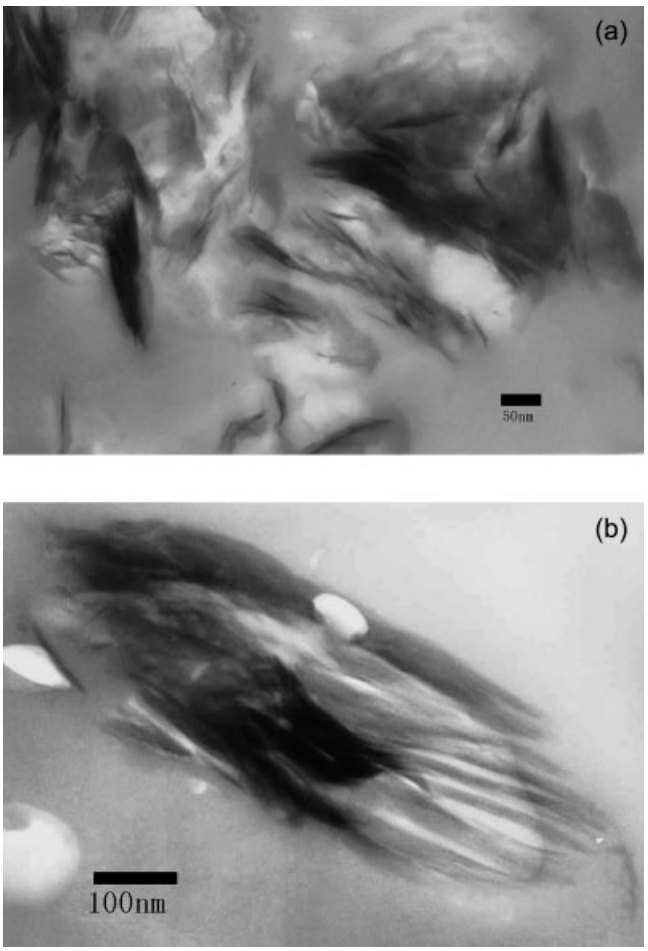

Figure 2 (a) TEM micrographs of CE/BT nanocomposites with various BT content: 1.0 wt %. (b) TEM micrographs of CE/BT nanocomposites with various BT content: 2.5 wt %.

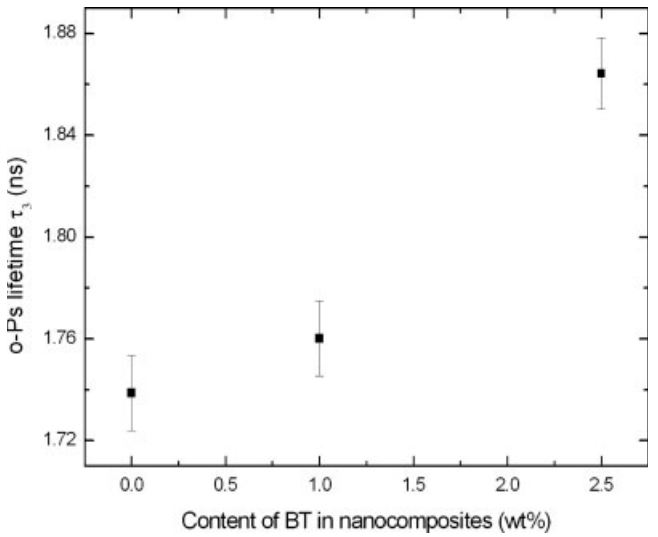

Figure 3 Content dependence of the *o*-Ps lifetime τ_3.

layers has been expanded from 1.4 to 3.1 nm. The broadening of the peak suggests that partial exfoliation occurred. From the TEM picture in Figure 2(b), we also found some aggregated states of BT.[8]

As mentioned above, we can conclude that the 1 wt % content nanocomposite has the best dispersed state. The sample with the best dispersion has the best toughing property (shown below).

The characterization by PALS

The filler content dependence of the *o*-Ps lifetime τ_3 and its intensity I_3 are shown in Figures 3 and 4, respectively. It is noteworthy that the longest lifetime τ_3 is not ascribed to *o*-Ps annihilation in defects of BT layer,[19] but attributed to *o*-Ps annihilation in matrix and interspacing of BT. Even though the *o*-Ps can annihilate in chains of organic-ions within interspacing of modified BT layer, the contribution from this phase in intercalated nanocomposite (with 2.5 wt % BT) is less than that in exfoliated nanocomposite (with 1 wt % BT), because the *o*-Ps is harder to access and annihilate in interspacing (between the gallery of unexfoliated BT layer) than in openspacing (covered the surface of exfoliated BT layer). So the increases of lifetime component τ_3 and its intensity I_3 can reflect the increase in size and concentration of the free volume holes in matrix. Using eq. (3), we can plot a curve about apparent free volume fraction against content of BT as shown in Figure 5. From Figure 5, it is very clear that the fractional free volume increases as the filler content is increased.

The changes in positron annihilation parameters can be explained as follows. When the organically modified BT was added into the CE system, the amine can influence the curing process. The carbon atom of the —OCN group is strongly electrophilic and hence is highly susceptible for attack by nucleophilic reagents.[1] The amine (hydrogen-donating impurity) can react straightforwardly with the cyanate groups to form four differently substituted triazines. In these heterocyclic triazine networks, the triazine rings are the branching points of the network and the higher the concentration, the higher the glass transition temperature.[20] With the low mass substituted triazines formed, the branching density of the thermosets is decreased, and the packing density of segments is lowered, which gives rise to the increase of mean size of free volume.

In addition, amine and sodium cations exchanged into BT gallery can catalyze the curing reaction of CE,[9,10] which results in the increase of the conversion of cure reaction and in the formation of more crosslinking structure, larger size of free volume,[21–23] and form, which makes the concentration of free volume holes (as measured by the PALS parameter I_3) increased.[21,23] So the apparent free volume fraction [calculated from τ_3 and I_3 by eq. (3)] increases with loading organically modified BT.

As mentioned above, our results are remarkably different from the results observed in other polymer nanocomposites, especially the intensity of *o*-Ps lifetime and free volume fraction.[24–26] For example, in the case of linear polymer/clay nanocomposites, the mean size of free volume holes does not vary significantly, and the concentration of free volume holes and the free volume fraction obviously decreases with the increase of the content of filler.[24,26] These changes in free volume properties of linear polymer-based nanocomposites may ascribe to the confine effect as follows. In the linear polymer-based nanocomposites, polymer chains are confined by interfacial layer, the intercalated or exfoliated layers can be

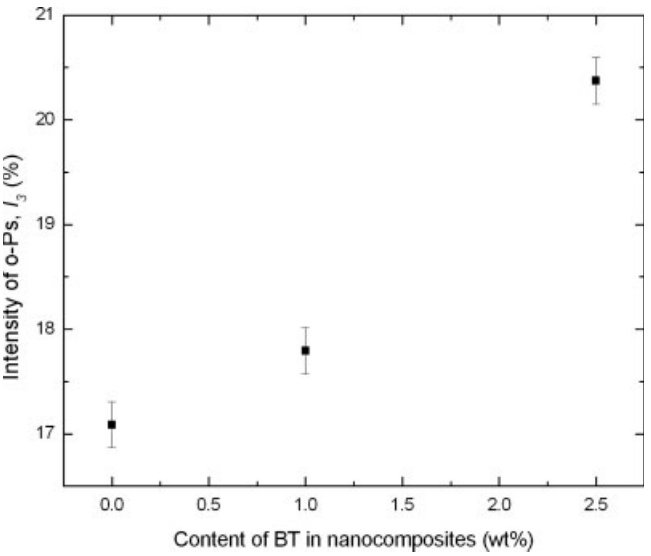

Figure 4 Content dependence of the *o*-Ps intensities.

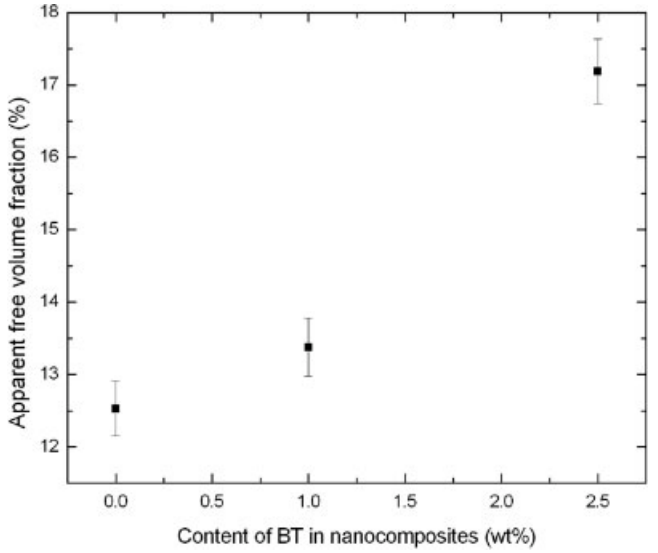

Figure 5 Content dependence of the apparent free volume fraction.

therefore be regarded as impermeable walls to restrict polymer chain conformations, and the polymer chains in interfacial region may be treated as adsorbed chains with one end attached to a plane, which is named tail chains.[27,28] The conformational number of confined chains is smaller than that in the free chains. Wu[29] calculated the conformational number of tail chains using the model of NRW (normal random walk) and deduced the ratio (α) of conformational number of the model tail chains to that of the free chains for linear polymer structure, as the segmental length $N \to \infty$, the ratio is

$$\alpha^{(d)}(N) \approx \frac{1}{\sqrt{2d\pi}} N^{-1/2} \tag{4}$$

where d is the dimension of the lattice. From this equation, the conformations reduced when the polymer chains were confined by nano-fillers, i.e., there is less room for the confined chain motion, thus the mobility of the confined polymer chains in the interfacial region was reduced by the nano-filler. Therefore, in the linear polymer/clay nanocomposites, the concentration of the free volume holes decreased.

However, in the case of thermosetting-based nanocomposites, the mobility of polymer chains could not be explained by above theory. Because in linear polymer chain system, the polymer chain (van der Waals attraction exists between chains) is relatively free and its mobility is easily confined by nano-layer. But in thermosetting-based nanocomposites, chains are restricted in the rigid network structure (in which chain units connect with chemical bond) and its mobility depend much more on the properties of network, such as the chemical structure and crosslinking density of network. The confined effect by nano-layer is weaker in thermosetting-based nanocomposites than that in linear polymer-based nanocomposites. The size and concentration of the free volume holes are mainly determined by the backbone structure, which strongly depended on the conversion of cure reaction.

Toughening behavior

The results of the impact strength test are shown in Figure 6. It is obvious that the impact strength reached the maximum value of 7.1 kJ/m^2 at 1 wt % BT, compared to 3.8 kJ/m^2 of pure CE and to 5.34 kJ/m^2 at 2.5 wt % BT. Some useful information about the fracture can also be observed from fractographic examination by SEM (have been published in previous article, Ref. 8). The pure CE basically shows a brittle fracture surface. Sample with 1 wt % BT shows a fracture surface consisting of narrow crevices and more particles (in smaller length), which are related to high toughness. Nanocomposite (with 2.5 wt % BT) with intercalated BT has a fracture surface consisting of wide crevices, which are related to moderate toughness.[8] The mechanical property can also be reflected by the results of the DMA. The patterns of the loss modulus clearly illustrate that all the samples have a relaxation peak as shown in Figure 7. The value of peak for the nanocomposite containing 1 wt % BT is the highest, the pure CE's relaxation peak is the lowest. The order of the peaks' height is in accord with the impact strength. Thus, we conclude that the exfoliated CE/BT nanocomposite (with 1 wt % BT) has the best toughness, and the intercalated CE/BT nanocomposite (with 2.5 wt % BT) also is tougher compared to the pure CE.[8]

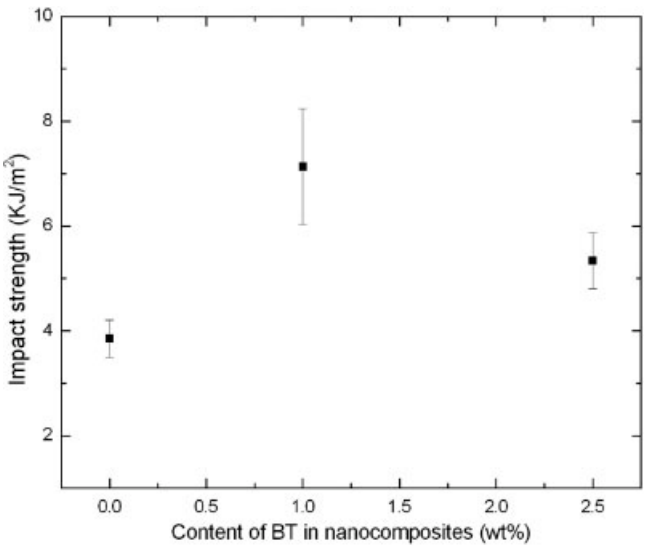

Figure 6 Impact strength of CE and CE/BT nanocomposites.

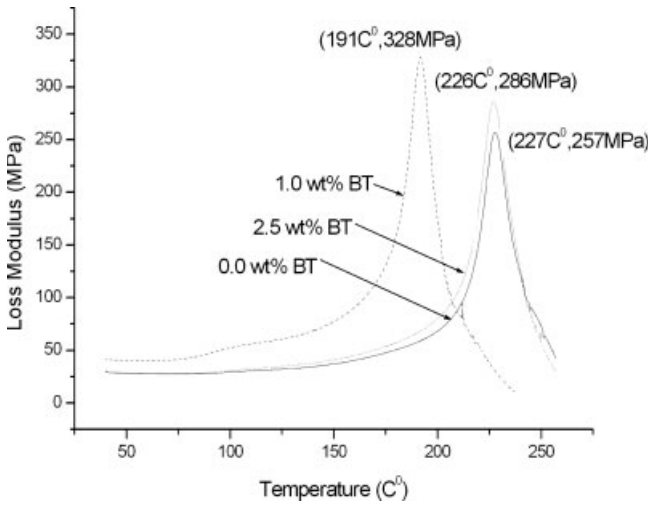

Figure 7 Loss modulus of CE and CE/BT nanocomposites.

It is reasonable that the apparent free volume fraction becomes larger when the organically modified BT insert into the CE system, which provides more room for the segmental motion, leading much impact energy to be absorbed.[30] So the CE/BT nanocomposites improve the toughness compared to the pure CE. However, the impact toughness does not increase monotonically with the increasing the apparent free volume fraction, because the morphology and the structure of the heterogeneities developed during the polymerization must be taken into account.[31] The exfoliated CE/BT nanocomposite has larger interfacial area and stronger interfacial interaction between the highly exfoliated clay and matrix, because the BT dispersed into the matrix homogeneously. These good interfacial properties (area and interaction) lead to the result that these materials can endure bigger deformation, indicating that this sample has the highest impact toughness.[32] However, in the intercalated CE/BT nanocomposite, the BT can not be uniformly dispersed into the matrix and even some aggregations can occur, which lead to smaller interfacial area compared to the exfoliated sample. The interfacial property can also reflect from the intensity of the second lifetime (I_2). The I_2 of the exfoliated one is 53.21%, which is bigger than the I_2 (= 48.58%) of the intercalated ones. Hence, the content of interfacial layers is bigger at 1.0 wt % BT.[17] The poorer interfacial property in the intercalated sample compared to the exfoliated sample results in decrease of the impact strength at 2.5 wt % BT.

Glass transition temperature

The glass transition temperature T_g is identified by DMA, as shown in Figure 7. According to the free volume theory, extra free volume should depress the T_g. However, the variation of T_g in our samples is not as expected, i.e., the nanocomposite with 2.5 wt % BT (have larger free volume fraction) has higher T_g than that in nanocomposite with 1 wt % BT. Becker et al.[25] also observed such similar phenomenon in studying the epoxy/silicate nanocomposites using PALS. As they reported that the mechanism of effects on T_g by clay is not fully understood, which may be the result of several factors. Sun et al.[33] revealed that the larger interfacial area induced by filler may depress the T_g. We may explain the unexpected result as follows. Firstly, the large interfacial area induced by good dispersion state in exfoliated nanocomposite (1 wt % BT content) depresses the T_g. Secondly, in high loading nanocomposite (2.5 wt % BT content), more amine and sodium cations (within the organic BT) can catalyze the curing reaction, which brings about the enhancement of the conversion of curing reaction and the formation of larger crosslinking network, therefore increase its glass transition temperature.[20] The detailed mechanism of effects on T_g by free volume and chemical structure needs further research.

CONCLUSION

The positron lifetime measurements reveal that the size and concentration of the free volume holes and the apparent free volume fraction increase with increasing the content of BT, which is because of the change in structure of triazine. With increasing the content of BT, the conversion of curing reaction enhanced due to its catalysis, and the higher the conversion of the curing reaction in curing process, the larger the free volume and fractional free volume. Experimental results also find that the free volume and the interfacial properties play an important role in determining the toughening behavior of CE/BT nanocomposites.

References

1. Reghunadhan Nair, C. P.; Mathew, D.; Ninan, K. N. Adv Polym Sci 2001, 155, 1.
2. Fang, T.; Shimp, D. A. Prog Polym Sci 1995, 20, 61.
3. Ganguli, S.; Dean, D.; Jordan, K.; Price, G.; Vaia, R. Polymer 2003, 44, 1315.
4. Ijima, T.; Yoshioka, N.; Tomoi, M. Eur Polym J 1992, 28, 573.
5. Hamerton, I., Ed. Chemistry and Technology of Cyanate Ester Resins; Chapman & Hall: London, 1994.
6. Giannelis, E. P. Adv Mater 1996, 8, 29.
7. Wang, Z.; Pinnavaia, T. J Chem Mater 1998, 10, 3769.
8. Feng, Y.; Fang, Z. P.; Mao, W.; Gu, A. J. J Appl Polym Sci 2005, 96, 632.
9. Wooster, T. J.; Abrol, S.; MacFarlane, D. R. Polymer 2004, 45, 7845.
10. Gangulia, S.; Dean, D.; Jordan, K.; Price, G.; Vaia, R. Polymer 2003, 44, 6901.
11. Pethrick, R. A. Prog Polym Sci 1997, 22, 1.
12. Wang, B.; Wang, Z. F.; Zhang, M.; Liu, W. H.; Wang, S. J. Macromolecules 2002, 35, 3993.

13. Jean, Y. C. Microchem J 1990, 42, 72.
14. Nakanishi, H.; Wang, S. J.; Jean, Y. C. In Positron Annihilation Studies of Fluid; Sharma, S. C., Ed.; World Scientific: Singapore, 1988; p 292.
15. Kirkgaard, P.; Eldrup, M.; Mogensen, O.; Petersen, N. J Comput Phys Commun 1981, 23, 307.
16. Wang, C. L.; Wang, S. J Phys Rev B 1995, 51, 8810.
17. Wang, S. J.; Wang, C. L.; Zhu, X. G.; Qi, Z. N. Phys Status Solidi A 1994, 142, 275.
18. Ray, S. S.; Okamoto, M. Prog Polym Sci 2003, 28, 1539.
19. Consolati, G.; Natali-Sora, I.; Pelosato, R.; Quasso, F. J Appl Phys 2002, 91, 1928.
20. Bauer, J.; Bauer, M. Macromol Chem Phys 2001, 202, 2213.
21. Hayashi, T.; Nakamura, H.; Suzuki T. Polymer 1999, 40, 1053.
22. Georjon, O.; Galy, J. Polymer 1998, 39, 339.
23. Venitti, R. A.; Gillam, J. K.; Jean, Y. C.; Lou, Y. J Appl Polym Sci 1995, 56, 1207.
24. Wang, Y. Q.; Wu, Y. P.; Zhang, H. F.; Zhang, L. Q.; Wang, B.; Wang, Z. F. Macromol Rapid Commun 2004, 25, 1973.
25. Becker, O.; Cheng, Y. B.; Varley, R. J.; Simon, G. P. Macromolecules 2003, 36, 1616.
26. Olson, B. G.; Peng, Z. L.; Srithwatpong, R.; McGervy, J. D.; Ishida, H.; Jamieson, A. M.; Manias, E.; Giannelis, E. P. Mater Sci Forum 1997, 255–257, 336.
27. Takahaski, A.; Kawagushi, M. Adv Polym Sci 1982, 48, 1.
28. Whittington, S. G. Adv Chem Phys 1982, 51, 1.
29. Wu, D. C. K. J Sci China Ser B 1996, 39, 608.
30. Jean, Y. C.; Deng, Q.; Nguyen, T. T. Macromolecules 1995, 28, 8840.
31. Rey, L.; Galy, J.; Sautereau, H.; Simon, G. P.; Cook, W. D. Polym Int 2004, 53, 557.
32. Jordan, J.; Jacob, K. I.; Tannenbaum, R.; Sharaf, M. A.; Jasiuk, I. Mater Sci Eng A 2005, 393, 1.
33. Sun, Y. Y.; Zhang, Z. Q.; Moon, K. S.; Wong, C. P. J Polym Sci Part B: Polym Phys 2004, 42, 3849.